Pergamon

Acta Materialia 50 (2002) 4369–4377

Acta MATERIALIA

www.actamat-journals.com

Combined effects of silica filler and its interface in epoxy resin

Haiying Wang [a,*], Yilong Bai [a], Sheng Liu [b], Jiali Wu [c], C.P. Wong [c]

[a] *LNM, Institute of Mechanics, Chinese Academy of Science, Beijing 100080, People's Republic of China*
[b] *Department of Mechanical Engineering, Wayne State University, Detroit, MI 48202, USA*
[c] *School of Materials Science and Engineering, Georgia Institute of Technology, Atlanta, GA 30332, USA*

Received 7 April 2002; received in revised form 2 July 2002; accepted 2 July 2002

Abstract

In this paper, mechanical properties of silica-filled epoxy resin are tested. The tests show that at elevated temperatures, the material's properties (e.g. yield stress, flow stress, etc.) vary immonotonically with filler volume fraction. Nano-indentation test results suggest that an interface region, stronger than the matrix, is formed in the materials. The formation of the interface has positive effects on the yield strengths of materials. The addition of particles in the matrix produces a large disturbance in stress distribution, leading to stress concentration in the matrix. The stress concentration has negative effects on the yield strengths of materials. The calculation demonstrates that the maximum stress in samples varies immonotonically with particulate concentration. So, the immonotonic variation of mechanical behavior of materials may be rooted in the contradictory effects of the interface region and the stress concentration caused by particulate addition.

Keywords: Composite; Mechanical properties; Interface; Hardness testing; Microstructure

1. Introduction

Rigid particulate filled polymeric materials are finding more and more grounds in microelectronic applications [1]. The materials studied in this paper are potential underfilling materials for the novel no-flow flip chip technology [2,3]. In this application, the material should meet the requirements for its curing conditions, shrinkage, adhesive and thermo-mechanical properties. Silica filled epoxy based materials are chosen as the most promising candidates because of their advantages such as low cost, adjustable curing temperature and curing rate by selecting a proper catalyst, and good adhesion to most of the substrate. However, it is reported that the epoxy resin without silica filler cannot meet the requirement for its thermo-mechanical properties, while the addition of silica filler will reduce the opportunity for solder bumps to contact copper pad during reflow [4]. Therefore, to enhance the thermo-mechanical properties without sacrificing the bonding yield, the filler size and concentration have to be carefully chosen.

* Corresponding author. Tel: +86-10-62545533 ext. 3004; fax: +86-10-62579511.

1359-6454/02/$22.00
PII: S1359-6454(02)00275-6

In the last few decades, many researchers have studied the mechanical properties of rigid particulate-filled polymeric materials [5–10]. The results show that the mechanical behavior of particulate-filled epoxy resins results from a complex interplay of properties of constituent phases. The principal relevant parameters are the volume fraction of filler, the particle size, the filler aspect ratio, the modulus and the strength of the filler, the resin–filler adhesion and the properties of the matrix. However, because of the complexity in specific materials, the influence of those parameters on the properties of underfill materials is at present incompletely understood. Improved understanding of the roles of these parameters could allow material designers to optimize the material constituents and microstructure design and to enhance material properties. The major concern of this paper is to study the effects of silica filler content on the mechanical behavior of a silica-filled epoxy resin. The results obtained in this paper will be helpful for the optimization of the material.

2. Experimental

2.1. Specimen preparation

The silica-filled epoxy resin composites employed in this study were supplied by Packaging Research Center, Georgia Institute of Technology. The samples were of the same resin matrix but were filled with spherical silica particulate by 0, 14, 21, 28, 33, and 39% filler volume fractions. The mean diameter of silica particulate was about 4 μm. The curing condition was 250°C for 40 min. To avoid the thickness effect, efforts were made to obtain thin, void-free sample sheets (about 0.40 mm) of uniform thickness during the process [11]. After the thin sheets were obtained, they were cut into thin-strip specimens using a diamond saw. The specimens were about 50 mm in length, 2.4 mm in width, and 0.4 mm in thickness. TMA tests show that the glass transition temperature (T_g) of these samples is about 150°C.

2.2. Mechanical test

In order to investigate the thermo-mechanical behaviors of such small specimens, a six-axis mini tester was developed at Wayne State University. This tester is automatically controlled by a microcomputer and easily operated under a Windows system. The mini tester is equipped with a chamber to heat or cool the specimen. To avoid bending or buckling effects, appropriate techniques were applied to ensure the specimen was clamped and aligned well [12].

Pure tensile tests of the thin-strip specimens were conducted on the six-axis mini-tester with fixed strain rate of 3.125×10^{-3}/s at ambient temperature, 50, 75, 100 and 115°C, respectively. Two to six specimens were tested under each testing condition to check the repeatability and consistency of test data.

3. Results

Fig. 1(a) and (b) are stress–strain curves of these specimens at ambient temperature and 115°C, respectively. These figures show that the mechanical behaviors of the materials are remarkably sensitive to the silica filler contents. Fig. 1(a) clearly shows that at room temperature, the materials become stronger with the addition of silica filler into the epoxy matrix. However, at 115°C (Fig. 1(b)), mechanical behaviors of materials vary immonotonically with increasing volume fraction of silica particulate.

Mechanical properties of the materials with different filler contents are compared in terms of Young's modulus, yield stress and flow stress. The Young's modulus is obtained from the initial slope of the stress–strain curve. Fig. 2 shows the variation of Young's modulus of the material with silica filler content at different testing temperatures. Generally, the addition of silica filler in the epoxy resin increases Young's modulus of materials. However, it is noticeable that at 115°C, the Young's modulus of the sample with 28 vol% silica is a bit lower than that of the sample with 14%.

For materials without obvious yielding points in their stress–strain curves, stresses at 0.2% inelastic

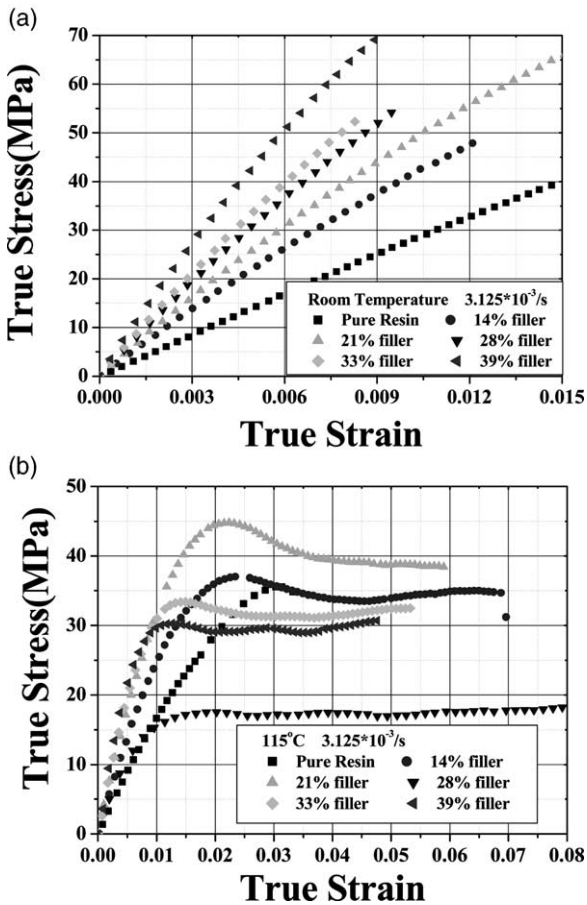

Fig. 1. Stress–strain curves obtained in pure-tensile test: (a) at ambient temperature, (b) at 115°C.

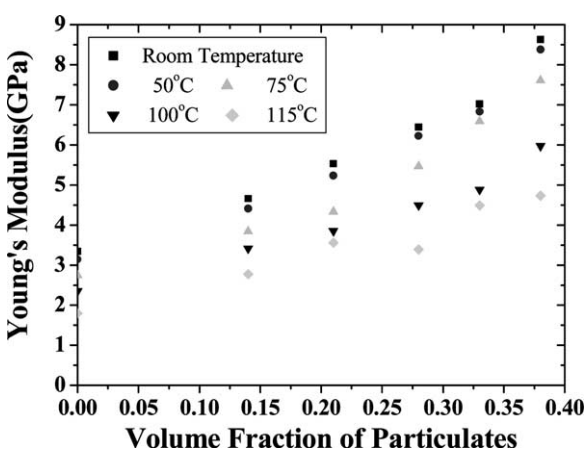

Fig. 2. Variation of Young's modulus with silica filler content.

strain, $\sigma_{p0.2}$, are chosen to compare. Fig. 3(a) illustrates the variation of $\sigma_{p0.2}$ with filler content under different testing conditions ($\sigma_{p0.2}$ under some conditions are not plotted because specimens break before the inelastic strains yield 0.2%.). At lower temperatures, $\sigma_{p0.2}$ increases with filler content increasing in the material. However, at high temperatures, the $\sigma_{p0.2}$ increases, then decreases, and increases again, with increasing filler content. The material with 14 or 21 vol% filler content has the highest $\sigma_{p0.2}$, while the material with 28 vol% silica has the lowest $\sigma_{p0.2}$. Fig. 3(b) and Fig. 4 show the variation of yield stress and flow stress of materials at 100 and 115°C. Obviously, both the yield stress and flow stress of materials vary in the same trend as $\sigma_{p0.2}$ does under these testing conditions.

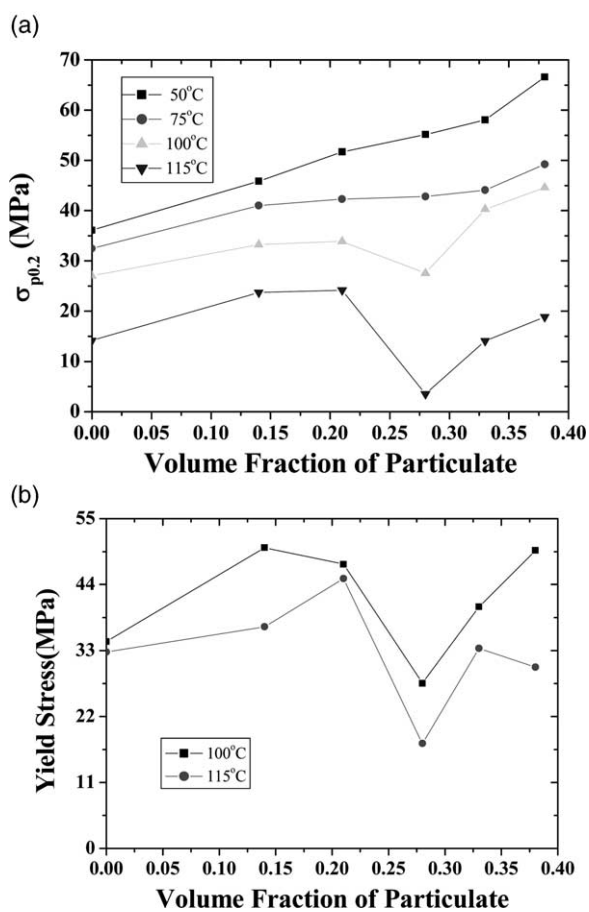

Fig. 3. Variation of (a) $\sigma_{p0.2}$ and (b) yield stress with silica filler content.

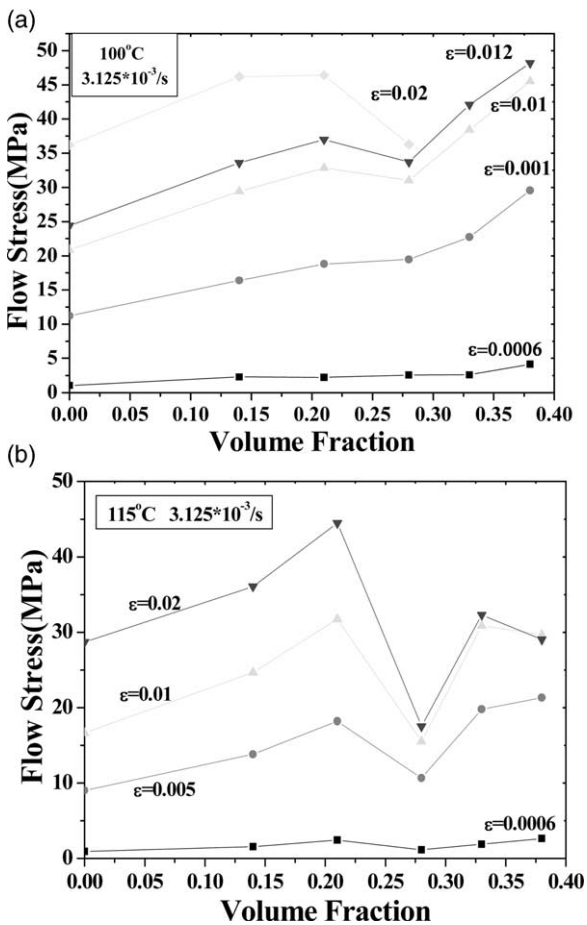

Fig. 4. Variation of flow stress with silica filler content: (a) at 100°C, (b) at 115°C.

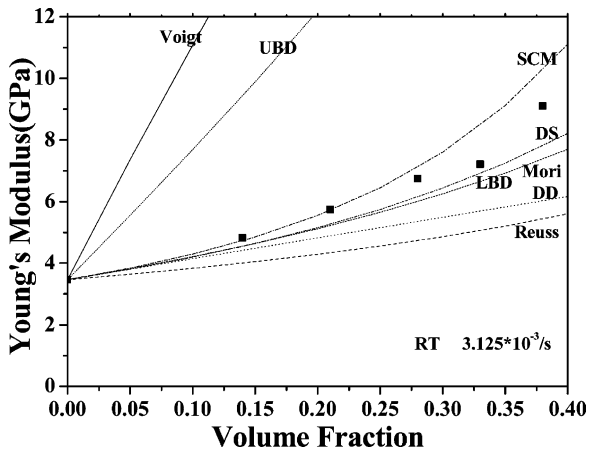

Fig. 5. Predicted Young's modulus vs. experimental data.

4. Discussion

4.1. Filler content effects on Young's modulus

The effect of the volume fraction of filler on the modulus of composites is well documented in the literature for a wide range of matrixes and filler materials [13–15]. Fig. 5 shows the comparison of predicted Young's modulus with experimental data. In Fig.5, MORI, UBD, SCM, LBD, DS, VOIGT, REUSS stand for the predicted results by the Mori–Tanaka method, the Hashin–Shtrikman upper bound, the Self-consistent method, the Hashin–Shtrikman lower bound, the Differential scheme, the Voigt estimate and the Reuss estimate, respectively. From this figure, it can be clearly seen that all models can give the increasing trend of Young's modulus with filler content. However, the error between model predictions and experimental data changes with different models. Generally, the Self-consistent method and the Differential scheme can provide relatively accurate prediction results.

Normally, the effective overall moduli of particulate-filled composites are determined by the moduli of constituent phases (particulates, matrix), the volume fraction of particulates, the interaction between the fillers and the matrix, as well as the interaction between particulate fillers [14]. The Reuss model and the Voigt model consider the interaction between the matrix and particulates by assuming that the stress (Reuss model) or strain (Voigt model) of each particulate (and hence the matrix) is equal to the applied stress or strain. Obviously, this assumption is too sketchy and cannot produce reliable predictions. With the help of the Eshelby tensor, the Dilute distribution method, the Hashin–Shtrikman variational principle and the Mori–Tanaka method include the interaction between the matrix and the embedded particulates exactly, but fail to take into account the interaction among particulates (which may not be negligible for large volume fractions of fillers). Thus, these methods only yield reasonable estimates of effective moduli when the volume fraction of particulates is relatively small. The Differential scheme assumes that the fillers are added into the matrix

gradually, with an infinitesimally small increment. The Dilute distribution assumption is used to obtain the new overall moduli. This process is continued until the final volume fraction of particulates is obtained. The Self-consistent method embeds the fillers in a fictitious unbounded homogeneous solid which has the as yet unknown overall properties, instead of those of the matrix. Therefore, in the Differential scheme and the Self-consistent method, the interaction of particles is included in some sense. In this study, these two methods provide more accurate predictions compared with other methods.

4.2. Filler content effects on yield stress and flow stress

The filler content effects on the plastic behavior of composites have been studied for many years. However, because of the complexity of the yielding mechanism of polymeric materials and the interaction between constituent phases, there is no widely applicable model for the prediction of plastic behavior of composites. Generally, the mechanical performance of reinforced plastic depends on the filler, the matrix, as well as the nature of the interface region. When particulate filler is added into the epoxy matrix, the interface region is formed as a result of the bonding between filler and matrix. The interface region may be a diffusion zone, a nucleation zone, a chemical reaction zone, and so forth, or any combination of the above. Since the mechanical property of the interface region may be different from that of the matrix, the formation of the interface region will affect the bulk properties of the composite. Alternatively, the addition of rigid particulates will incur stress-concentration or damage in the matrix, which has a weakening effect on the composite's properties. The mechanical effect produced by filling-in rigid particles is dependent on the combining results incurred by the above two facts. In the next few paragraphs, we will examine these effects caused by the addition of filler into the matrix.

4.2.1. Interface properties characterization

Although it is very difficult to properly represent the interface region quantitatively in theoretical models, modern instruments do provide methods for us to get information about the existence and properties of the interface region.

The interfacial bonding conditions of these materials were investigated by the fractograph analysis method. The specimens were dipped into liquid nitrogen and then broken so that the fracture surface could be examined using SEM. Typical micrographs of the fracture surfaces are shown in Fig. 6. Although the fracture surfaces get rougher with increasing silica filler in the materials (Fig. 6), there was no evidence of any form of inelastic deformation in the fracture surface. This indicates that the matrix is very brittle at very low temperatures. In addition, there is no evidence of particle–matrix debonding in all the figures, which suggests that the silica particles are well bonded to the matrix and the broken was matrix dominated.

As a comparison, the fracture surfaces of specimens at 115°C were examined using SEM. Fig. 7 depicts the micrographs at 115°C. In this figure, the matrix near the silica particles is obviously stretched, showing that the matrix is very ductile at 115°C. In addition, all bare particles on the fracture surfaces are covered by a thin layer of matrix. This indicates that in the process of crack propagation, the particulate cannot be separated from the matrix, thus the crack has to "climb over" these particles, which supports the foregoing conclusion of strong interfacial bonding.

The mechanical properties of interface region were tested with Nano Indenter II made by MTS Instrument. A detailed description of the instrument is available elsewhere (www.mts.com/nano).

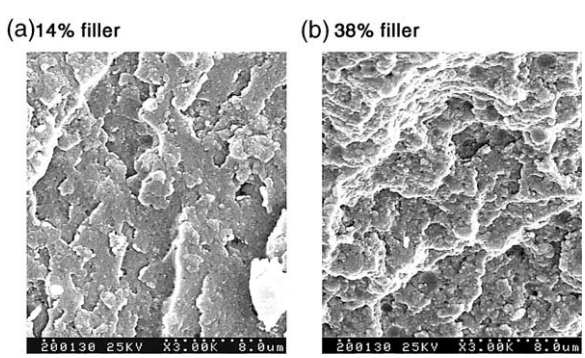

Fig. 6. Typical micrographs of the fracture surfaces at low temperature.

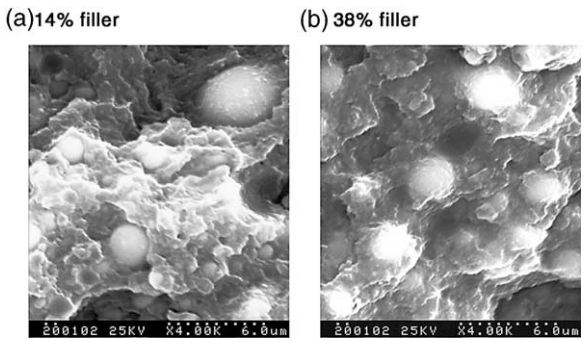

Fig. 7. Typical micrographs of the fracture surfaces are shown at 115°C.

The test was conducted on specimens with 14 and 38 vol% filler content. The indentation depth and the distance between adjacent indentations were set at 500 nm and 3.75 μm. After the test, the hardness–depth curves were obtained. Generally, the hardness–depth curves fall into three categories (Fig. 8). As shown in Fig. 8, there are three hardness plateaus (7.44, 1.82, 0.4GPa) in these curves. After comparing the hardness values with data obtained in other tests [16], it can be concluded that the hardness values of silica filler and epoxy resin are about 7 and 0.4 GPa, respectively. As a result, we deduce the hardness of the interface region is about 1.82 GPa, falling between those of the epoxy matrix and the silica filler.

The SEM observation and Nano-Indenter test show that the interface regions are stronger than the matrix. Therefore, the deformation of the matrix surrounding the particles will be constrained by fillers, which has a strengthening effect on the composite's bulk properties. The more filler added into the matrix, the more interface region is formed in the material; as a result, the stronger the composite will be. Therefore, considering only the strengthening effect of the interface region, the relationship between the yield stress and the volume fraction of filler is schematically plotted as curve A in Fig. 9.

4.2.2. Stress field analysis

Micromechanical methods, such as the Eshelby Effective Inclusion Method (EIM) [13], have been applied with great success to the stress and strain field analysis of inhomogeneous materials. In this paper, the Eshelby EIM is used to analyse the stress/strain field in a specimen under pure tensile loading.

Consider an infinitely extended material with the elastic moduli C^0_{ijkl} containing ellipsoidal inclusions with the elastic moduli C^{I}_{ijkl}. With the Eshelby EIM and Mori–Tanaka theory, the equivalent inclusion equation and stress equilibrium equation can be given as [13]:

$$C^{\mathrm{I}}_{ijkl}(\varepsilon^0_{kl} + \bar{\varepsilon}_{kl} + S_{klmn}\varepsilon^*_{mn}) = C^0_{ijkl}(\varepsilon^0_{kl} + \bar{\varepsilon}_{kl} + S_{klmn}\varepsilon^*_{mn} - \varepsilon^*_{mn}) \quad (1)$$

$$C^0_{ijkl}\bar{\varepsilon}_{kl} + fC^0_{ijkl}(S_{klmn}\varepsilon^*_{mn} - \varepsilon^*_{kl}) = 0 \quad (2)$$

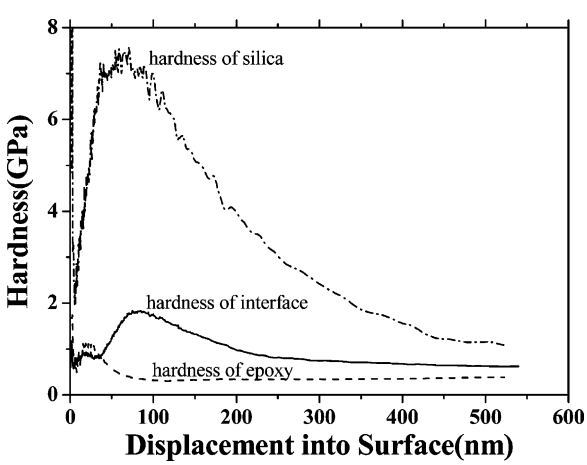

Fig. 8. Three typical hardness–depth curves.

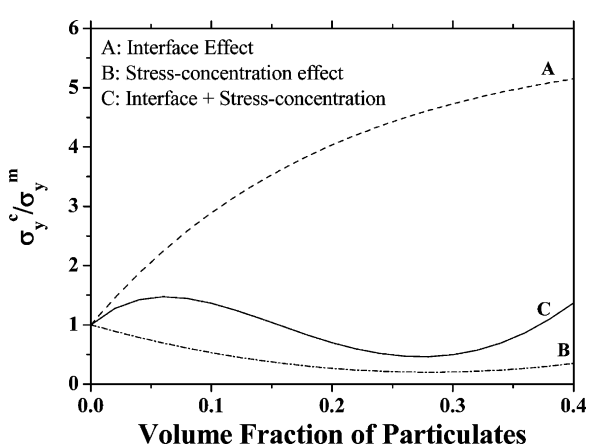

Fig. 9. Predicted yield stress vs. the volume fraction of filler.

where f is the volume fraction of inclusions, $\bar{\varepsilon}$ is the average strain disturbance in the matrix caused by the addition of inclusions, $\varepsilon*$ is the eigenstrain, and S is the Eshelby tensor.

The stresses in the inclusions σ_{ij}^{I} and matrix σ_{ij}^{m} are obtained as:

$$\sigma_{ij}^{I} = C_{ijkl}^{I}(\varepsilon_{kl}^{0} + \bar{\varepsilon}_{kl} + S_{klmn}\varepsilon_{mn}^{*}) = C_{ijkl}^{0}(\varepsilon_{kl}^{0} + \bar{\varepsilon}_{kl} + S_{klmn}\varepsilon_{mn}^{*} - \varepsilon_{mn}^{*}) \quad (3)$$

$$\sigma_{ij}^{m} = C_{ijkl}^{0}(\varepsilon_{kl}^{0} + \sum_{q=1}^{N} D_{ijkl}^{q}(x)\varepsilon_{mn}^{*}) \quad (4)$$

where D_{ijkl}^{q} is extended Eshelby tensor.

It is assumed that the spherical silica particulates are uniformly distributed in the specimen, thus, the stress and strain distribution in the specimen can be represented by the model shown in Fig. 10. The model is loaded uniaxially along x_1 direction. In order to investigate the effect of particle concentration on the stress field, different values of a/l are used, where a is the radius of the filler, and l is the distance between the nearest particles. The volume fraction of particles can be calculated from:

$$f = \frac{4\pi a^3}{3l^3} \quad (5)$$

Since the stress disturbance in the matrix caused by particles decreases significantly with the particle spacing increasing, disturbance from particulates within a distance less than $10a$ are considered in the calculation. In order to take the effect of temperature into consideration, the ratio of Young's modulus of matrix and particulates, E_p/E_m, is assumed to be 10, 20, 30, 40 and 50. The Poisson ratio of matrix and particulates is assumed to be 0.38 and 0.16, respectively. The stress distribution around particles was obtained from Eqs. (1)-(5).

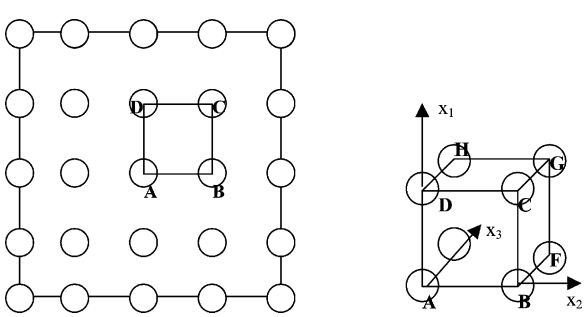

Fig. 10. Computational model for stress field analysis.

Fig. 11 shows for the assumed E_p/E_m studied, the variation of maximum stress σ_{11} in the matrix with particulate concentration. It is demonstrated that adding particulates into the matrix will cause stress concentration in the material and the maximum stress in the matrix differs with the particulate concentration. However, more particulate filling does not always result in higher maximum stress in the matrix. The maximum stress in the matrix varies immonotonically with filler content. The material with 25–30 vol% filler undergoes the highest stress in the matrix. Based on the calculation, the variation of silica filler content not only leads to different maximum stress in the matrix, but also to the variation of the matrix volume which undergoes higher stress. For materials with different filler content ($E_p/E_m = 30$), the fractions of the matrix volume undergoing higher stress are compared, as shown in Fig. 12. Obviously, for material with 20–30 vol% filler, more area of matrix undergoes higher stress compared to materials with other filler contents.

If maximum stress is one of the major reasons for the material's yielding, the stress analysis results show that the filler content affects the yield and plastic behavior immonotonically. Therefore, the weakening effect caused by the stress concen-

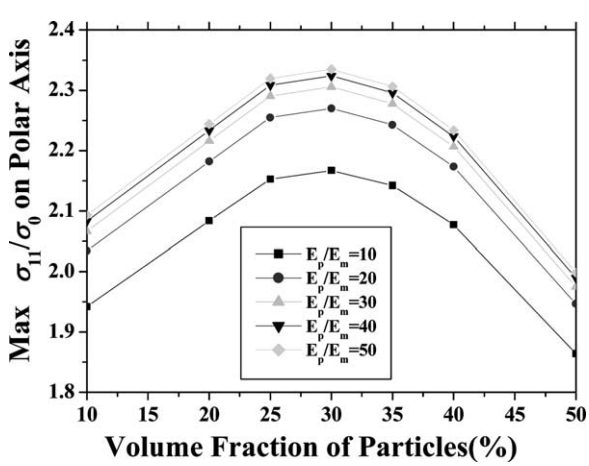

Fig. 11. Variation of maximum stress σ_{11} in the matrix with particulate concentration.

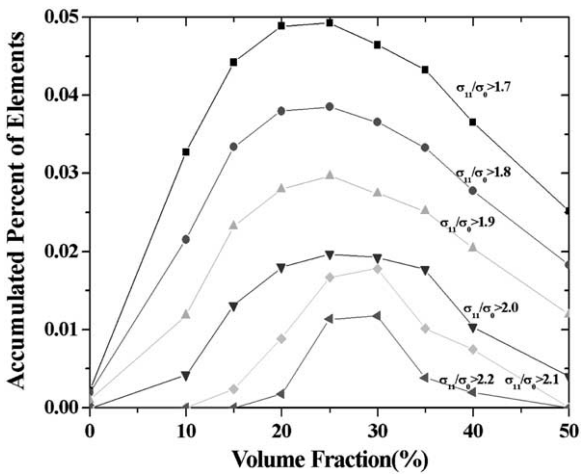

Fig. 12. Volume undergoing higher stress in the model vs. particulate concentration: (a) at ambient temperature, (b) at 115°C.

tration gives a relationship between the yield stress and the volume fraction of the filler, schematically plotted as curve B in Fig. 9.

Considering both the weakening effect caused by the stress concentration and the strengthening effect caused by the interface region, we can sketch curve C in Fig. 9, which qualitatively agrees with experimental data at elevated temperatures.

5. Conclusions

1. The addition of silica particulates into epoxy resin can remarkably alter the material's mechanical properties. The material properties (Young's modulus, yield stress, etc.) increase with the increasing filler content at low temperatures. However, at elevated temperatures, the material properties (e.g. yield stress, flow stress, etc.) vary immonotonically with particulate volume fraction.
2. The Nano-indentation test results suggest that an interface region, stronger than the matrix, is formed in the materials. The formation of a stronger interface region has positive effects on the yield strengths.
3. The addition of particles to the matrix produces a large disturbance of stress distribution, leading to stress concentration in the matrix. The calculation demonstrates that the maximum stress in samples varies immonotonically with particulate concentration. The stress concentration has negative effects on the yield strengths of materials.
4. The immonotonic variation of mechanical behavior of materials may be rooted in the contradictory effects of the interface region and the stress concentration caused by particulate addition.

Acknowledgements

The authors are grateful to Professor Mengfeng Xia and Dr Taihua Zhang for useful discussions and suggestions in this work. The research is financially supported by the Chinese Academy of Sciences (KJCX2-SW-L2), National Science Foundation of China, National Science Foundation White House Presidential Fellowship, and Semiconductor Research Cooperation.

References

[1] Wong CP. Polymers for electronic and photonic applications. Boston: Academic Press, 1993.
[2] Wong CP, Shi SH, No-flow underfill of epoxy resin, anhydride, fluxing agent and surfactant. US patent 6180696; Jan 2001.
[3] Shi SH, Wong CP. High performance no flow underfills for low-cost flip-chip applications. In: Proceedings of the 47th Electronic Components and Technology Conference. San Jose, CA: Institute of Electrical and Electronics Engineers; 1998. p. 117.
[4] Shi SH, Wong CP. IEEE Trans Electronics Packaging Manufacturing 1999;22:331.
[5] Harismendy I, Miner R, Valea A et al. Polymer 1997;38:5573.
[6] Cantwell WJ, Smith JW, Kausch HH et al. J. Mater. Sci 1990;25:633.
[7] Cantwell WJ, Roulin-Moloney AC, Kaiser T. J. Mater. Sci. 1988;23:1615.
[8] Koh S, Kim J, Mai Y. Polymer 1993;34:3446.
[9] Shin DK, Lee JJ. A study on the mechanical behavior of EMC and thermal stress analysis in plastic packaging. In: Advances in electronic packaging, EEP-vol 19-1. ASME; 1997. p. 253.
[10] Swanson F, Gregornik N. Modern Plastics 1972;3:106.
[11] Ren W, Qian Z, Liu S. Scale effect on packaging materials. In: Proceedings of the 49th Electronic Compo-

nents and Technology Conference, San Diego, CA. 1999. p. 1229.
[12] Lu M, Qian Z, Ren W et al. Int J Solids Struct 1999;36:65.
[13] Mura T. Micromechanics of defects in solids, 2nd ed. Martinus Nijhoff Publishers, 1987.
[14] Nemat-Nasser S, Hori M. Micromechanics: overall properties of heterogeneous materials. North-Holland Press, 1993.
[15] Hashin Z, Shtrikman S. J Mech Phys Solids 1963;11:127.
[16] Zhang T, Yang Y. Modern Scientific Instruments 2002;1:32.